



Cite this: DOI: 10.1039/d5im00385g

## Recyclable semi-EV sulphur cured natural rubber elastomer composites

Thomas Griggs,<sup>a</sup> Anureet Kaur,<sup>a</sup> Meet M. Fefar,<sup>a</sup> Keizo Akutagawa,<sup>a</sup> Ton Peijs,<sup>b</sup> Biqiong Chen<sup>c</sup> and James J. C. Busfield<sup>\*a</sup>

Natural rubber (NR) has been widely vulcanised for most practical engineering applications using sulphur for the last 180 years, however, the crosslinked network significantly inhibits recyclability. Minimising reduction in performance after recycling is essential in developing a more circular economy within the rubber industry. Previously, this research group exploited controlled inhibition of the disulphide metathesis, through addition of copper(ii) methacrylate (CuMA) to the compound, enabling significant recyclability of rubber waste in conventionally vulcanised (CV) NR networks. CV networks predominantly contain poly- and di-sulphide crosslinks, however, in practice, a greater proportion of rubber products are made exploiting the more thermally stable efficient vulcanising (EV) or semi-efficient vulcanising (SEV) sulphur crosslinking systems. This work demonstrates that by optimising the CuMA concentration, inhibition of the disulphide metathesis works well with the most widely exploited SEV system. A CuMA concentration of 0.62 phr enabled excellent recyclability, providing excellent mechanical properties in materials post recycling up to very large recycled rubber content. It is demonstrated the system also achieves high recyclability using a model SEV tyre compound including 50 phr carbon black filler. This discovery opens the opportunity to recycle the 15 million tonnes of elastomer materials within tyre waste produced globally each year.

Received 22nd December 2025,  
Accepted 3rd April 2026

DOI: 10.1039/d5im00385g

rsc.li/icm

Keywords: Recycling; Sustainability; Disulphide bonds; Chemical inhibitors; Selective breakdown; Natural rubber.

## 1 Introduction

Used in a very large array of applications such as fashion, mining, automotive and healthcare, the global application of natural rubber (NR) exceeded 15 million tonnes in 2024.<sup>1</sup> Harvested from *Hevea Brasiliensis* trees, in 2024 16.3 million tonnes of NR were produced from Southeast Asia, with countries like Thailand, Indonesia, and Vietnam being major contributors.<sup>2,3</sup> Although NR is bio-sourced, therefore renewable, the sustainability of harvesting practices is a growing concern. Traditional methods often lead to deforestation, loss of biodiversity, and soil degradation.<sup>4</sup> The demand for NR is primarily driven by the automotive industry, where it is extensively used in the manufacture of tyres due to its high durability and abrasion resistance. Tyre

production alone accounts for about 70% of the total worldwide NR consumption.<sup>5</sup>

Tyres generally consist of complex blends of a range of rubbers, most commonly NR or styrene butadiene rubber (SBR), with several additional components, including metal reinforcements and fillers, such as carbon black (CB) or silica. Generally, the tyre itself consists of about 50% rubber of which the composition between SBR and NR will vary depending on the location in the tyre and the expected use of the tyre. Passenger car tyres typically contain a higher proportion of SBR, while off-road and truck tyres show a much higher amount of NR.<sup>6</sup>

Prior to crosslinking, NR and SBR do not show the properties required to match the tyre application, therefore these types of thermosetting elastomers need to be cross-linked before use. This is carried out by adopting a vulcanisation reaction that utilises either peroxide, or more commonly elemental sulphur. This vulcanisation reaction involves heating the uncured rubber to high temperatures, generally around 150 °C, alongside a curing package involving elemental sulphur, in the case of sulphur vulcanisation, and an accelerator.

While crosslinking is a necessity for achieving the property requirement of the targeted application, it severely

<sup>a</sup> School of Engineering and Materials Science, Queen Mary University of London, Mile End Road, London, E1 4NS, UK. E-mail: j.busfield@qmul.ac.uk

<sup>b</sup> Centre for Polymer and Composite, WMG, University of Warwick, Coventry, CV4 7AL, UK

<sup>c</sup> Department of Chemistry, University of Liverpool, Crown Street, Liverpool, L69 7ZD, UK



hinders the recyclability of the products, as all the polymer chains are permanently connected. All thermosetting polymers have issues with recycling. For NR elastomer matrix composites, whose primary application lies in the tyre industry, the main focus within the literature has been on the recycling of tyres themselves. Since landfilling of tyres has been legislated against globally, methods of recycling have improved. Examples include pyrolysis or energy recovery, which involve controlled combustion of tyres in an inert atmosphere.<sup>7,8</sup> While both show promise, there are inherent downsides as only about a quarter of the energy is recovered, while several hazardous gases and chemicals are released as byproducts.<sup>9</sup> Another commonly seen end-of-life option for tyres is crumbing, which involves breaking down the tyres into significantly smaller particulate to be utilised for alternative purposes such as construction materials or as flooring for either sports fields or children's playgrounds.<sup>10,11</sup> More recent developments in the recycling of NR and tyres have seen several different methodologies developed to selectively break down the sulphur crosslinks, resulting in a material which can be reutilised with limited reductions in properties. Some such methodologies include chemical, ultrasonic, microwave or specialised milling processes.<sup>12–15</sup>

The crosslinking reaction links the rubber molecules with permanent sulphur bridges of varying lengths, ranging from monosulphide and disulphide bonds to longer polysulphide bonds. The length of these sulphur bridges is heavily reliant on the curing ingredients used during vulcanisation, specifically the ratio between accelerator and sulphur used. A conventional cure system (CV) results when there are higher levels of sulphur and a lower amount of accelerator, with around 95% of the resulting crosslink bridges being either poly- or disulphides.

When lower levels of sulphur and higher levels of accelerator are used, an efficient vulcanisation system (EV) is seen, in this case typically around 80% of the resulting crosslink bridges are monosulphides. An intermediate state is achieved with a semi-efficient cure system (SEV), where the sulphur and accelerator amounts are roughly equal, and this produces about 50% polysulphide bridges.<sup>16</sup> The cure system is specifically designed, depending upon the intended application, CV systems show a high toughness due to the

longer polysulphide crosslinks yielding and reforming under high strains, however these systems are also more susceptible to thermal degradation, resulting in worse ageing properties. While EV systems show significantly improved ageing due to the abundance of more stable monosulphide crosslinks, they also show lower strength. SEV systems show a compromise between these two systems by incorporating both good ageing and strength performance, and it is therefore widely used in a large range of applications, such as the tyre industry. Initial work was carried out on a CV system, as the largest number of target crosslink lengths would be present, showing high recyclability.<sup>17</sup> This paper extends this work investigating the much more widely used SEV system.

Unfilled rubber is not widely used in industry, as it rarely meets the demands of the application, with CB being the most utilised reinforcing filler for engineering rubber products. Depending on the colloidal properties of the CBs used, a large range of properties, such as the dynamical mechanical or stress-strain properties can be significantly enhanced. The filler also plays a significant role in the energy dissipation of the rubber as well as heat build-up.<sup>18</sup> Therefore, to be commercially relevant to most elastomer products and to fully understand the recyclability through the mechanisms proposed herein, it is vital to test this recycling approach on a typical elastomeric system, which in this case is a semi-EV cured NR compound filled with CB.

In the current work, initial studies were carried out on simple unfilled SEV systems. Copper(II) methacrylate (CuMA) was introduced to the formulation package to act as an inhibitor for the disulphide metathesis. This inhibitor is intended to suppress the disulphide exchange at service temperature but allow for rearrangement under high temperature shear reprocessing. CuMA was added at five different ratios (Table 1) of moles CuMA in relation to the moles of disulphide bonds calculated from the formulation recipes to understand the inhibitor's capability of recycling an SEV system containing fewer disulphide bonds. Further investigations are made into the inhibitor's effectiveness within SEV systems filled with CB, to understand whether the inhibition process is still effective in combination with the added surface chemistry of the CB particles.

**Table 1** Rubber formulations in phr

/phr	SEV control	SEV CuMA-1/1	SEV CuMA-1/2	SEV CuMA-1/4	SEV CuMA-1/8	SEV CuMA-1/16	SEV control CB	SEV CuMA 1/16 CB
NR	100	100	100	100	100	100	100	100
ZnO	3.5	3.5	3.5	3.5	3.5	3.5	3	3
StA	2.5	2.5	2.5	2.5	2.5	2.5	3	3
IPPD	2	2	2	2	2	2	—	—
6PPD	—	—	—	—	—	—	1	1
TMQ	—	—	—	—	—	—	1	1
Sulphur	2.5	2.5	2.5	2.5	2.5	2.5	1.5	1.5
CBS	2.5	2.5	2.5	2.5	2.5	2.5	0.8	0.8
TMTD	—	—	—	—	—	—	0.8	0.8
CuMA	—	9.89	4.94	2.47	1.24	0.62	—	0.62
CB	—	—	—	—	—	—	50	50



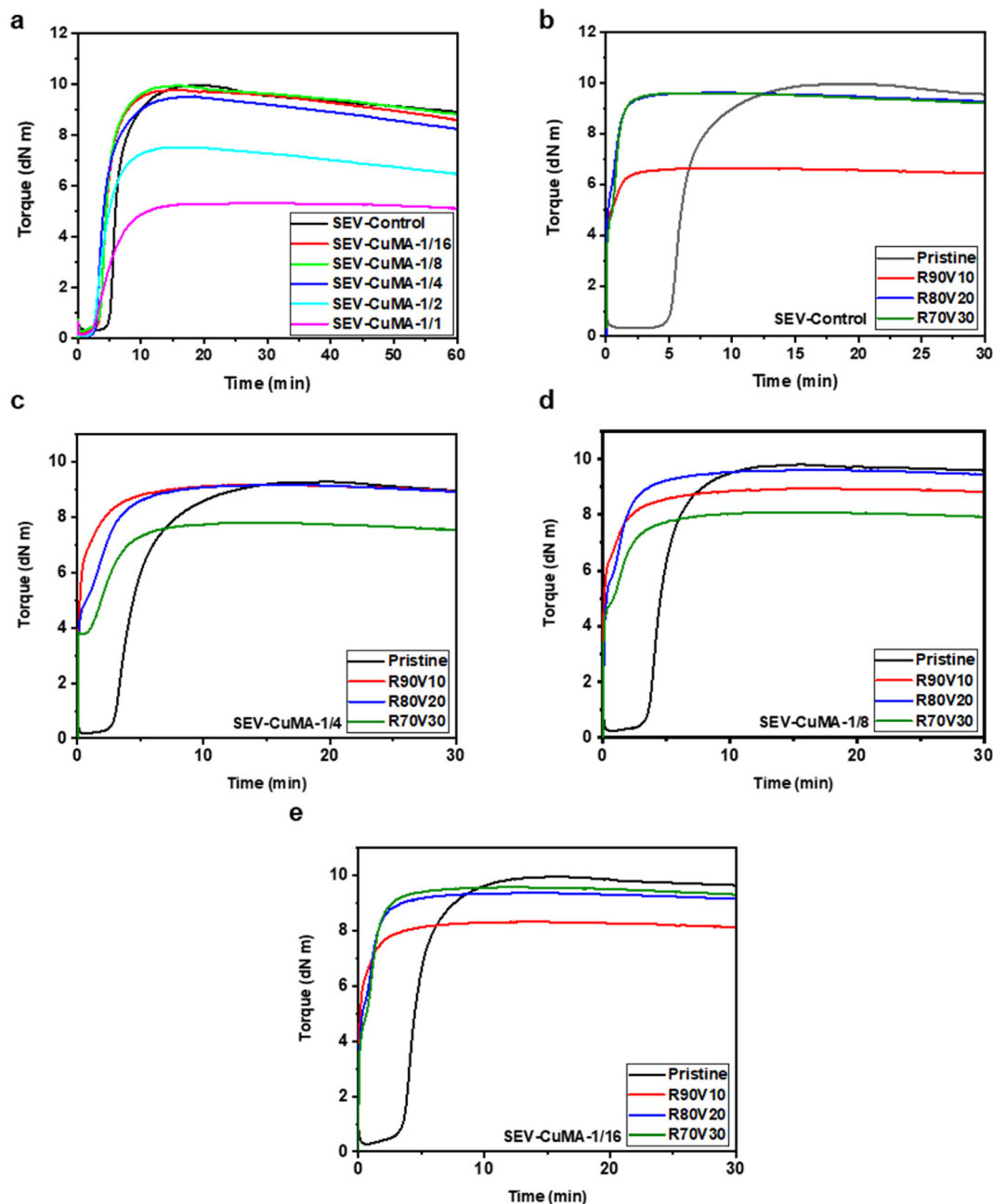


**Fig. 1** MDR analysis at 150 °C for 60 min. (a) Comparison between SEV-control (solid black line), SEV-CuMA-1/16 (solid red line), SEV-CuMA-1/8 (solid green line), SEV-CuMA-1/4 (solid blue line), SEV-CuMA-1/2 (solid light-blue line), and SEV-CuMA-1/1 (solid magenta line); curing characterisation of recycled compounds at 150 °C for 30 min. MDR analysis comparison between pristine (solid black line) and recycled compounds R90V10 (solid red line), R80V20 (solid blue line) and R70V30 (solid green line): (b) SEV-control, (c) SEV-CuMA-1/4, (d) SEV-CuMA-1/8 and (e) SEV-CuMA-1/16.

## 2 Results and discussion

To check the curing characteristics of the SEV systems, MDR analysis was performed at 150 °C (Fig. 1a).

Initial testing was conducted on SEV-CuMA-1/1, SEV-CuMA-1/2, and SEV-CuMA-1/4 to compare with the previously reported CV systems,<sup>17</sup> however it was noted that an increase in the amount of CuMA resulted in a reduction of the maximum torque values seen in MDR, which was assumed to be a reduction in the crosslink density of the materials. As 1/

4 showed the highest properties, and the aim of this study was to develop recyclable materials without sacrificing the good mechanical properties associated with SEV systems a further decrease in the ratio was evaluated at 1/8 and 1/16.

Torque measurements showed very similar properties of both the pristine and recycled compounds, with a very minor reduction in scorch time seen for 1/16, while recycling efficiencies of tensile properties showed 1/16 resulted in improved recovery of properties, while also utilising significantly less CuMA, resulting in reduced cost. From these



factors it was considered that 1/16 showed the most promise. Additionally, in SEV-CuMA-1/4 and SEV-CuMA-1/8 the maximum torque rankings do not correspond to the rankings of virgin material added to recycle, which could be attributable to a lack of control of the disulphide metathesis. In the case of SEV-CuMA-1/16, the expected hierarchy is seen between virgin content and maximum torque, once again suggesting this is the optimal concentration of those tested. Further optimisation of the inhibitor to disulphide ratio is planned for future investigation.

One assumption as to why a lower concentration works more efficiently in the SEV system is the alteration of the crosslink rankings compared to the CV systems, where less polysulphides are present. From literature, inhibitors can reduce polysulphides into disulphides.<sup>19</sup> Potentially, the disulphide bond is exploited for recycling, in the CV system a higher concentration of CuMA is required for the increased amount of disulphides, whereas in the SEV system, a higher concentration of disulphides is already present, so the CuMA is only needed for stabilisation.

The further reduction of CuMA concentration resulted in near identical final torque values to the control sample. Conversely, within the previously reported CV systems, the addition of CuMA inhibitor did not appear to provide the material with any improved reversibility properties when compared to the control compound.<sup>17</sup> The recycled compounds were classified as R90V10, R80V20 and R70V30, with R referring to the reclaimed content and V referring to the virgin content. Therefore, R90V10 is 90% reclaimed 10% virgin. Evaluation of each recycled compound for all of SEV-control, SEV-CuMA-1/16, SEV-CuMA-1/8, and SEV-CuMA-1/4 was once again carried out using MDR analysis at 150 °C for 30 min, to understand scorch time, torque recovery, and reversion characteristics (Fig. 1b–e).

One drawback to the recycling methodology is that a reduction in scorch time is noticed for the recycled compounds, limiting the potential reprocessing techniques. Some potential

routes to address this include the introduction of scorch retarders into the cure package to introduce a longer processing window to accommodate for processing such as injection moulding. An additional route involves utilising a more selective breakdown of the initial compound, such as S3M, which has been seen to allow for improved scorch times in recycled system, even without the addition of any disulphide metathesis inhibitors.<sup>15</sup>

As expected, SEV-control showed the lowest torque recovery with the highest reclaimed content. However, no difference in torque values were observed between R80V20 and R70V30 (Fig. 1b). Each of the recycled compounds with CuMA showed relatively good reversion control, showing a stable maximum torque value, as well as showing good torque recovery with as high as 90% reclaimed content, with these values effectively reaching the same torque as the pristine material. Similarly to the previously reported CV systems, there was still very little recovery of the scorch time within the recycled materials, suggesting that the materials once again do not flow like the uncured equivalent after the reclaiming process, even with the addition of CuMA. Further investigation is still required to promote an increase in scorch time to widen the processing window for the compound. Interestingly, in the case of both SEV-CuMA-1/4 (Fig. 1c) and SEV-CuMA-1/8 (Fig. 1d) the compound containing the highest ratio of virgin material, in this case 30%, showed the lowest achieved torque values, while SEV-CuMA-1/16 showed, as expected, lowest torque recovery for R90V10, and minimal difference between R80V20 and R70V30 (Fig. 1e).

Crosslink density calculations report the highest  $v_{\text{phy}}$  for SEV-control, reaching  $1.95 \times 10^{-4} \pm 8.13 \times 10^{-6} \text{ mol cm}^{-3}$ . While the addition of CuMA at 1/16, 1/8 and 1/4 concentration,  $v_{\text{phy}}$  drops to  $1.61 \times 10^{-4} \pm 6.00 \times 10^{-7} \text{ mol cm}^{-3}$ ,  $1.66 \times 10^{-4} \pm 9.35 \times 10^{-7} \text{ mol cm}^{-3}$ , and  $1.60 \times 10^{-4} \pm 1.34 \times 10^{-6} \text{ mol cm}^{-3}$  respectively (Fig. 2a). Recycled compounds show increasing  $v_{\text{phy}}$  as reclaimed compound content is increased from 70%, to 80%, and 90%, as R90V10 reaches  $v_{\text{phy}}$  of  $2.20 \times 10^{-4} \pm 5.83 \times 10^{-6}$

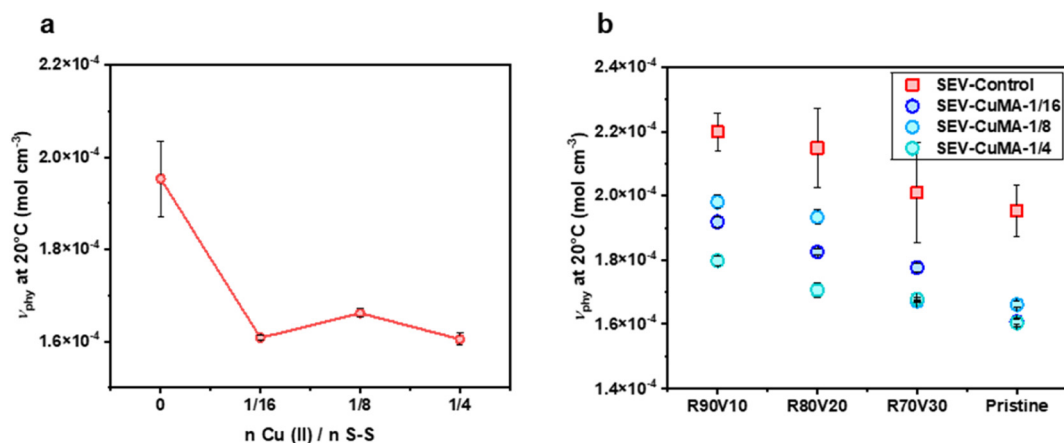
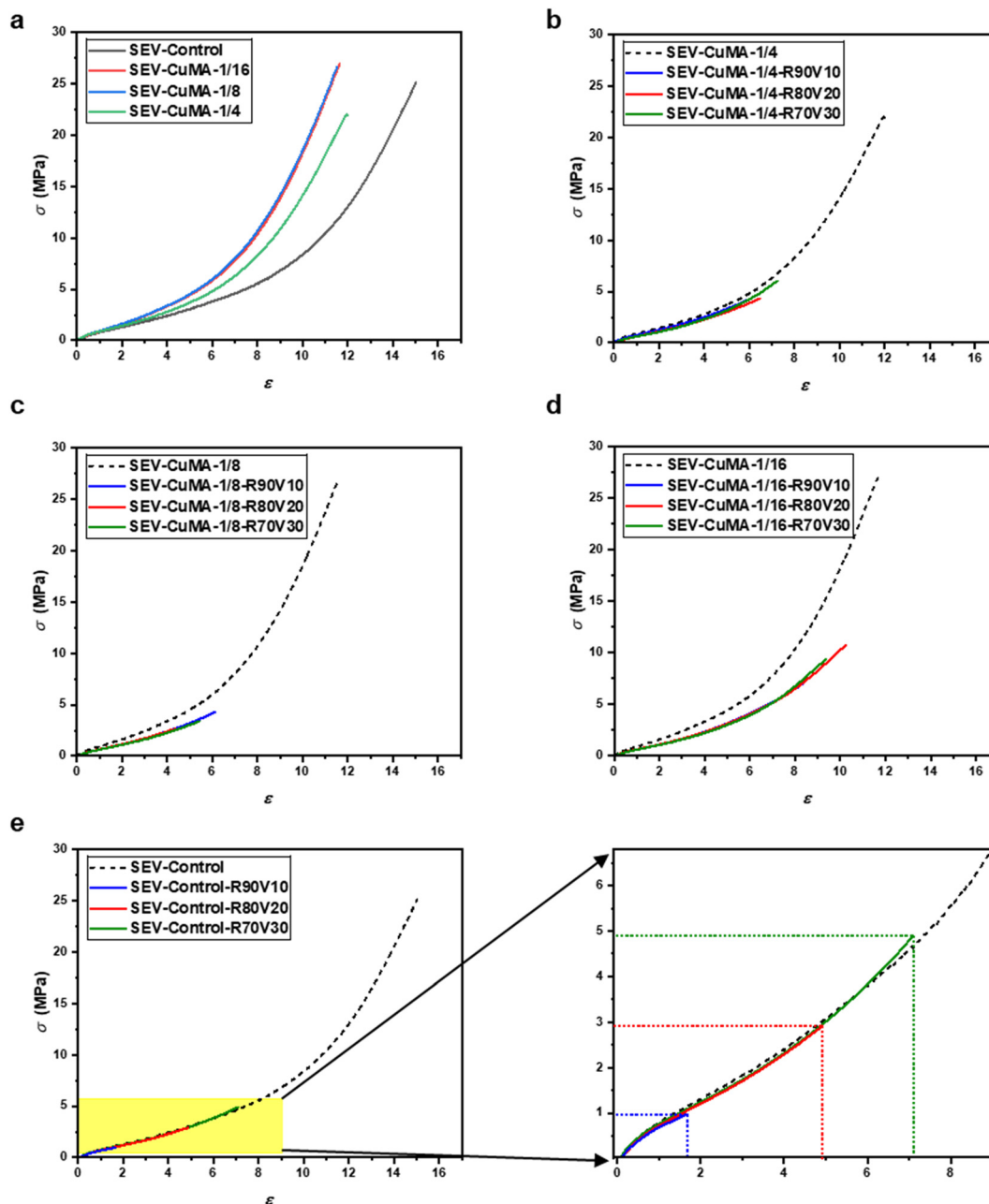


Fig. 2 Crosslink density calculations for the unfilled compounds. (a) Pristine-cured compounds (solid red line with red filled circles); (b) recycled compounds of SEV control (red filled squares), SEV-CuMA-1/16 (dark blue filled circles), SEV-CuMA-1/8 (light blue filled circles), and SEV-CuMA-1/4 (green aquamarine filled circles). Standard deviations are reported with black lines.





**Fig. 3** Stress–strain curves from tensile tests of pristine-cured compounds. (a) Comparison between SEV-control (solid black line), SEV-CuMA-1/16 (solid red line), SEV-CuMA-1/8 (solid blue line), and SEV-CuMA-1/4 (solid green line). Stress–strain curves from tensile test of recycled compounds; comparison between typical tensile curves of pristine (short dash black line), R90V10 (solid blue line), R80V20 (solid red line), and R70V30 (solid green line): (b) SEV-CuMA-1/4, (c) SEV CuMA 1/8, (d) SEV CuMA 1/16 and (e) SEV-control with zoomed in plot for clarity.

$\text{mol cm}^{-3}$  for SEV-control,  $1.91 \times 10^{-4} \pm 1.66 \times 10^{-6} \text{ mol cm}^{-3}$  for SEV-CuMA-1/16,  $1.98 \times 10^{-4} \pm 2.14 \times 10^{-6} \text{ mol cm}^{-3}$  for SEV-CuMA-1/8, and  $1.80 \times 10^{-4} \pm 1.45 \times 10^{-6} \text{ mol cm}^{-3}$  for SEV-CuMA-1/4 (Fig. 2b).

To understand the mechanical behaviour of the pristine-cured compounds, uniaxial tensile testing was carried out (Fig. 3). The stress–strain curves suggest that the addition of CuMA significantly increases the stiffness of the materials, while also decreasing the elongation at break, potentially suggesting lower sulphur rank crosslinks in the materials as

well as a decrease in crosslink density, which can be verified utilising sulphur rank analysis in future works (Fig. 2b). Alternative explanations could include variations in the network heterogeneity resulting in areas with distinctly lower stiffness, or changes in the polymer filler interactions with the addition of CuMA in the system.

The ranking in terms of increasing stiffness follows SEV-control, showing maximum  $\epsilon$  and  $\sigma$  values of  $14.5 \pm 0.9$  and  $24.8 \pm 3.9 \text{ MPa}$  respectively, followed by SEV-CuMA-1/4, reporting maximum  $\epsilon$  of  $11.9 \pm 0.1$  and  $\sigma$  of  $25.2 \pm 2.1$



MPa, and then SEV-CuMA-1/8, showing maximum  $\varepsilon$  of  $11.7 \pm 0.1$  and  $\sigma$  of  $26.5 \pm 0.7$  MPa, and finally SEV-CuMA-1/16, reporting maximum  $\varepsilon$  of  $11.8 \pm 0.2$  and  $\sigma$  of  $26.5 \pm 0.7$  MPa. SEV-CuMA-1/4 shows slightly reduced mechanical properties when compared to SEV-CuMA-1/8 and SEV-CuMA-1/16.

It should also be noted that there appears to be very little difference between the mechanical performance of CuMA 1/8 and CuMA 1/16. For each formulation containing CuMA it is apparent that significantly improved recycling ability is achieved when compared to SEV-control, which only showed notable recovery, once a ratio of 30% uncured compound was introduced (Fig. 3e). It can be noted that the breakdown method utilised involved only heating up the materials and passing them through the two-roll mill, requiring no additional harmful chemicals, while also releasing no byproducts during the recycling process as can be produced in some alternative recycling methods.<sup>9</sup> As the concentration of CuMA is reduced from 1/4 to 1/8 and then 1/16, the stiffness of the recycled compounds reduces, suggesting a slight reduction of the cross-link density after recycling. (Fig. 3c–e). However, little difference in the stiffness is observed as the uncured compound content is increased from 10% to 30%. The only noticeable increase is in the maximum  $\varepsilon$  and  $\sigma$  values achieved as uncured compound content is increased to 30% achieving the highest properties: with values of  $6.6 \pm 1.8$  and  $4.6 \pm 1.8$  MPa,  $8.4 \pm 0.7$  and  $7.4 \pm$

1.1 MPa,  $6.3 \pm 2.1$  and  $4.9 \pm 2.5$  MPa and  $8.2 \pm 1.2$  and  $7.1 \pm 1.8$  MPa for SEV-control, SEV-CuMA-1/4, SEV-CuMA-1/8 and SEV-CuMA-1/16 respectively. For better visualisation, recycling efficiency calculations are also reported (Fig. 4). As observed from the tensile test data, SEV-control recycling efficiencies are lower than CuMA containing compounds, in R90V10 a recycling efficiency for stress ( $\eta_\sigma$ ) of  $3.4 \pm 0.8\%$  and a recycling efficiency of strain at break ( $\eta_\varepsilon$ ) of  $10.4 \pm 2.1\%$  was reached, while in R80V20 a  $\eta_\sigma$  of  $9.5 \pm 3.7\%$  and a  $\eta_\varepsilon$   $27.1 \pm 9.8\%$  was achieved, and in R70V30  $\eta_\sigma$  of  $18.7 \pm 7.8\%$  and  $\eta_\varepsilon$   $45.4 \pm 12.8\%$  was reached (Fig. 4a). SEV-CuMA-1/4 reported the highest efficiency, as in R90V10  $\eta_\sigma$  of  $27.7 \pm 9.7\%$  and a  $\eta_\varepsilon$  of  $68.0 \pm 14.0\%$  was reached, while in R80V20 a  $\eta_\sigma$  of  $21.7 \pm 9.5\%$  and a  $\eta_\varepsilon$  of  $60.1 \pm 14.7\%$  was achieved, and in R70V30 a  $\eta_\sigma$  of  $29.6 \pm 4.8\%$  and a  $\eta_\varepsilon$   $70.4 \pm 6.1\%$  was reached (Fig. 4a).

SEV-CuMA-1/8 reported the lowest efficiencies among the CuMA containing compounds, as in R90V10 a  $\eta_\sigma$  of  $13.2 \pm 4.5\%$  and a  $\eta_\varepsilon$  of  $44.7 \pm 11.8\%$  was reached, while in R80V20 a  $\eta_\sigma$  of  $14.9 \pm 9.6\%$  and a  $\eta_\varepsilon$  of  $46.0 \pm 18.9\%$  was achieved, and in R70V30 a  $\eta_\sigma$  of  $18.4 \pm 9.6\%$  and a  $\eta_\varepsilon$  of  $54.2 \pm 18.4\%$  was reached (Fig. 4c). SEV-CuMA-1/16 reported comparable trends to SEV-CuMA-1/4, as in R90V10 a  $\eta_\sigma$  of  $17.3 \pm 9.0\%$  and a  $\eta_\varepsilon$  of  $51.7 \pm 20.0\%$  was reached, while in R80V20  $\eta_\sigma$  of  $27.7 \pm 13.6\%$  and  $\eta_\varepsilon$   $67.5 \pm 21.2\%$  was achieved, in R70V30 a  $\eta_\sigma$  of  $26.7 \pm 6.8\%$  and a  $\eta_\varepsilon$  of  $69.6 \pm 10.4\%$  was reached (Fig. 4d). While following the initial stress–strain curve

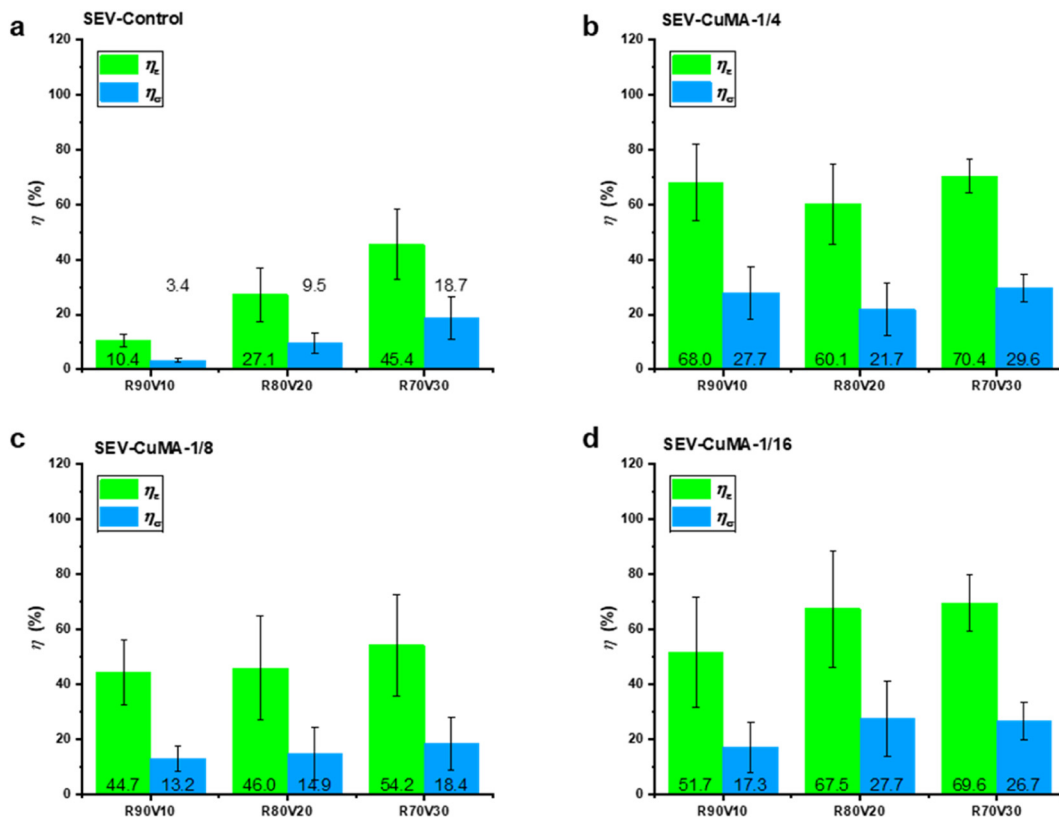


Fig. 4 Recycling efficiency in terms of stress and strain of recycled compounds. Results for: (a) SEV-control, (b) SEV-CuMA-1/4, (c) SEV-CuMA-1/8 and (d) SEV-CuMA-1/16. Green bars for  $\eta_\varepsilon$ , blue bars for  $\eta_\sigma$ , standard deviation in solid black line.



closely, the reduction in properties can partially be a result of the larger particle size seen in the recycled rubber, potentially increasing the intrinsic flaw size which has a large impact on strength properties.<sup>20</sup> Given the relatively good recovery of SEV-CuMA-1/16 recycled compounds, it was determined that further research with 50 phr CB-filled formulations be carried out solely utilising a 1/16 ratio between CuMA and disulphide bonds (Table 1).

The curing characteristics of CB-filled compounds were found using MDR analysis (Fig. 5a). Very similar initial stages are seen with and without CuMA, with near identical minimum torque values, before the compound without CuMA undergoes a slightly faster curing, before reaching a maximum torque value of 21 dN m. It can be noted that the inhibitor-containing compound shows an increased maximum torque at 22 dN m, once again suggesting that the cross-link density is slightly increased with the presence of CuMA. In both cases a slight marching cure can be seen, with the torque slowly rising throughout the 30 minute curing period.

It should be noted that for the CB filled compounds, only two recycle loadings were investigated, R90V10 and R50V50. The recycled compounds both with and without CuMA show good reversion control with reasonable recovery

of torque for both recycle loadings (Fig. 5b and c). The compound with CuMA shows a higher level of recovery for maximum torque, as well as a slightly lower minimum torque, suggesting the formulation is more capable of initial flow when compared to the case with no CuMA present. In the case of R50V50, there is a very short processing window with a similar scorch time to the pristine curve. Crosslink density calculations show SEV-control-CB has a physical crosslinking density ( $v_{\text{phy}}$ ) at  $2.27 \times 10^{-4} \pm 9.84 \times 10^{-6} \text{ mol cm}^{-3}$ , while adding CuMA slightly increases this value to  $2.33 \times 10^{-4} \pm 4.62 \times 10^{-6} \text{ mol cm}^{-3}$  (Fig. 5d).

In both cases a recycling event shows a decrease in the crosslink density, with SEV-control-CB showing values of  $2.16 \times 10^{-4} \pm 4.55 \times 10^{-6} \text{ mol cm}^{-3}$  and  $1.87 \times 10^{-4} \pm 4.38 \times 10^{-6} \text{ mol cm}^{-3}$  for R90V10 and R50V50 respectively. SEV-CuMA-1/16-CB shows good consistency in crosslink density post recycling with R90V10 showing a value of  $1.85 \times 10^{-4} \pm 6.39 \times 10^{-6} \text{ mol cm}^{-3}$  and R50V50 showing the same value of  $1.85 \times 10^{-4} \pm 1.55 \times 10^{-6} \text{ mol cm}^{-3}$ .

Similarly to the unfilled compound (Fig. 3) the addition of CuMA to the formulation appears to result in slightly higher crosslinking levels, seen through a stiffening of the materials at higher strain ratios. This is also suggested by the MDR

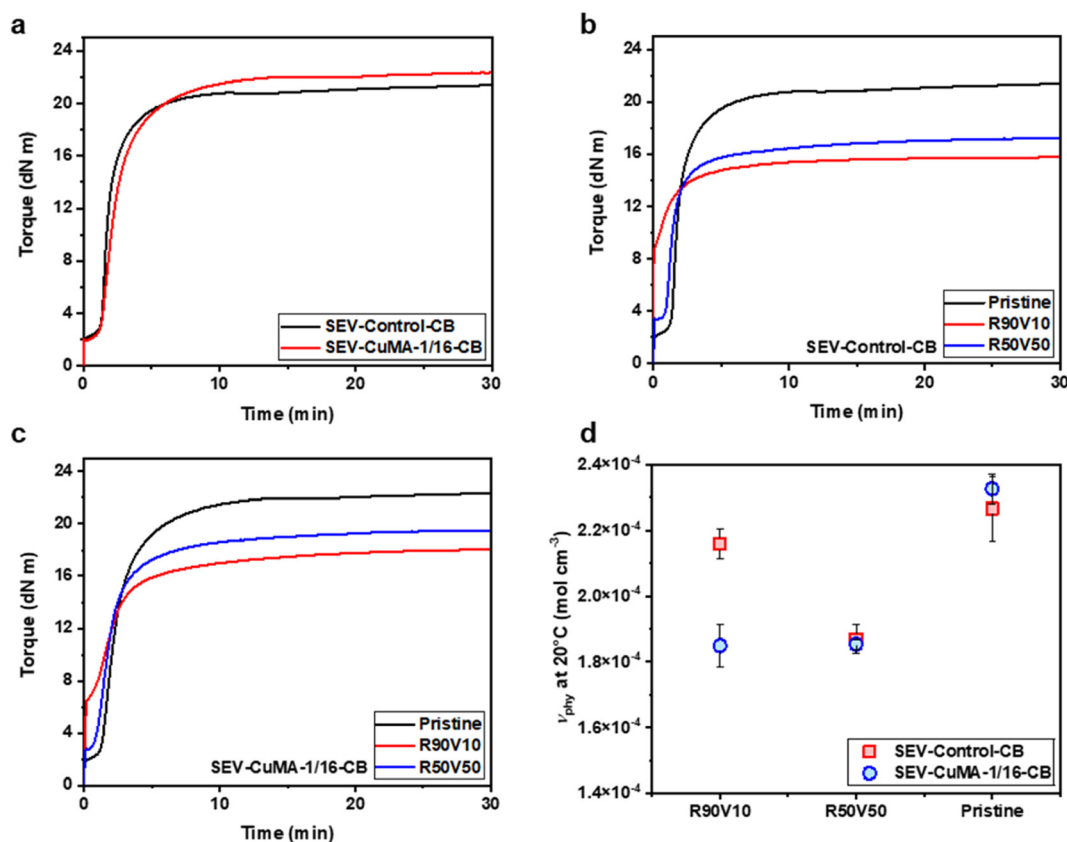


Fig. 5 MDR analysis at 150 °C for 30 min of CB-filled pristine-cured compounds. (a) Comparison between SEV-control-CB (solid black line) and SEV-CuMA-1/16-CB (solid red line); curing characterisation of CB-filled recycled compound. MDR analysis at 150 °C for 30 min of recycled compounds of (b) SEV-control-CB pristine (solid black line), R90V10 (solid red line), and R50V50 (solid blue line); (c) SEV-CuMA-1/16-CB pristine (solid black line), R90V10 (solid red line), and R50V50 (solid blue line). Crosslinking density calculations for filled compounds; (d) recycled compounds of SEV-control-CB (red filled squares), SEV-CuMA-1/16-CB (dark blue filled circles).



traces (Fig. 5) where the compound with CuMA shows a higher final torque value. SEV-CuMA-1/16 CB shows maximum strain and stress values of  $5.9 \pm 0.2$  and  $24.6 \pm 0.6$  MPa respectively, while SEV-control-CB shows maximum values of  $6.7 \pm 0.1$  and  $24.1 \pm 0.5$  MPa (Fig. 6a). In both cases, these are within the range commonly seen within formulations utilised within tyres.<sup>21,22</sup> A significant difference can be seen regarding the compound with and without CuMA, with the latter performing considerably worse

(Fig. 6b and c), it could be hypothesised that the reduction of properties could be a result of the recycled material forming poor interfaces with the virgin material. This could be verified through a type of fatigue peeling tests, as carried out by Baumard *et al.*<sup>23</sup>

SEV-control-CB showed a significant reduction in elongation at break in R50V50 with  $\epsilon$  of  $4.2 \pm 0.3$  and in R90V10 with  $\epsilon$  of  $3.3 \pm 0.5$ , however, with a much sharper increase in stiffness, although only reaching in R50V50  $\sigma$  of

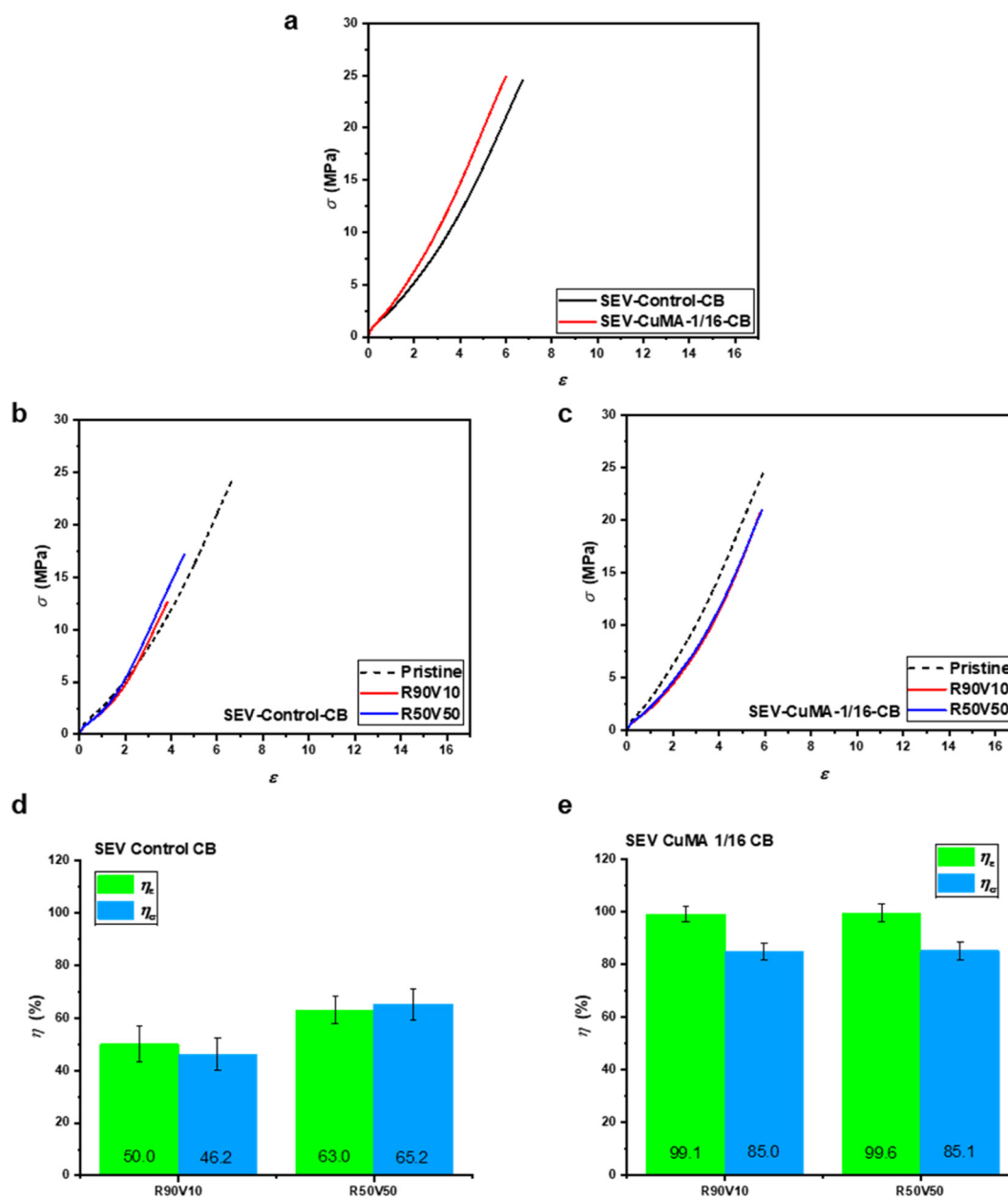


**Fig. 6** Stress-strain curves from tensile tests of CB-filled pristine-cured compounds. (a) Comparison between SEV-control-CB (solid black line) and SEV-CuMA-1/16-CB (solid red line); stress-extension ratio curves from tensile test of CB-filled pristine-cured and recycled compounds: typical tensile test curves of (b) SEV-control-CB pristine (short dash black line), R90V10 (solid red line), R50V50 (solid blue line) and (c) SEV-CuMA-1/16-CB pristine (short dash black line), R90V10 (solid red line), R50V50 (solid blue line); recycling efficiency in terms of stress and strain of CB filled recycled compounds. Results for: (d) SEV-control-CB R90V10 and R50V50 (e) SEV-CuMA-1/16-CB R90V10 and R50V50 (green bars for  $\eta_\epsilon$ , blue bars for  $\eta_\sigma$ , standard deviation in solid black line).



15.7 ± 1.4 MPa and in R90V10 with  $\sigma$  of 11.1 ± 1.5 MPa. In the case of SEV-CuMA-1/16-CB, a slight reduction in stiffness is seen, as the elongation at break is almost identical, reaching in R50V50  $\epsilon$  of 5.8 ± 0.1 and in R90V10  $\epsilon$  of 5.9 ± 0.1, however, a slight reduction in maximum stress is seen, as in R50V50  $\sigma$  of 20.9 ± 0.7 MPa was reached and in R90V10  $\sigma$  of 20.9 ± 0.6 MPa was achieved (Fig. 6c). This reduction in the overall stiffness of the recycled materials is hypothesised to be attributable to changes in filler networking, as reported in previous literature.<sup>15</sup> Future testing to validate this hypothesis could include carrying out Payne effect characterisation to understand variations in the filler network, or bound rubber measurements, to understand how CuMA alters the chemically bound rubber. It is assumed that the sulphur crosslink distribution remains similar for the inhibited systems, whereas in the control sample, an increase in modulus is seen, suggesting that the filler network breakdown softening effect is less than the increase resulting from a redistribution of sulphur crosslinks to lower ranks introducing additional crosslinks within the system. The little difference between R90V10 and R50V50 of SEV-CuMA-1/16-CB suggests that good recyclability can be achieved when using very minimal amounts of virgin material.

It can be noted that the carbon black filled compounds show a higher overall efficiency when compared to the

unfilled formulations. This could be hypothesised to be a collaborative effect between the carbon black surface acting as a radical trap before the CuMA then stabilises the sulphur radicals, resulting in less lost radicals and more efficient disulphide metathesis.<sup>24</sup>

To easily understand the recycling efficiency, both  $\eta_\sigma$  and  $\eta_\epsilon$  of the recycled materials were calculated according to eqn (6) and (7) respectively (Fig. 6d and e). It can be noted firstly that high efficiencies are achieved for SEV-CuMA-1/16-CB compared to SEV-control-CB, as SEV-CuMA-1/16-CB-R90V10 reached a  $\eta_\sigma$  of 85.0 ± 3.2% and a  $\eta_\epsilon$  of 99.1 ± 2.9% and SEV-CuMA-1/16-CB-R50V50 reached a  $\eta_\sigma$  of 85.1 ± 3.4% and a  $\eta_\epsilon$  of 99.6 ± 3.4%, while SEV-control-CB-R90V10 reached a  $\eta_\sigma$  of 46.2 ± 6.2% and a  $\eta_\epsilon$  of 50.0 ± 6.8% and SEV-control-CB-R50V50 reached a  $\eta_\sigma$  of 65.2 ± 5.8% and a  $\eta_\epsilon$  of 63.0 ± 5.1%. The lower standard deviations reported for SEV-CuMA-1/16-CB suggest that better reproducibility has been achieved when CuMA is incorporated.

Additionally, there is very little difference in efficiency with increasing uncured compound content from 10% to 50% with CuMA, whereas a reasonable increase in both maximum stress and strain values was achieved for SEV-control-CB as the uncured compound content increased from 10% to 50%. This is a significant increase to the current state of art within recycling of filled natural rubber compounds,

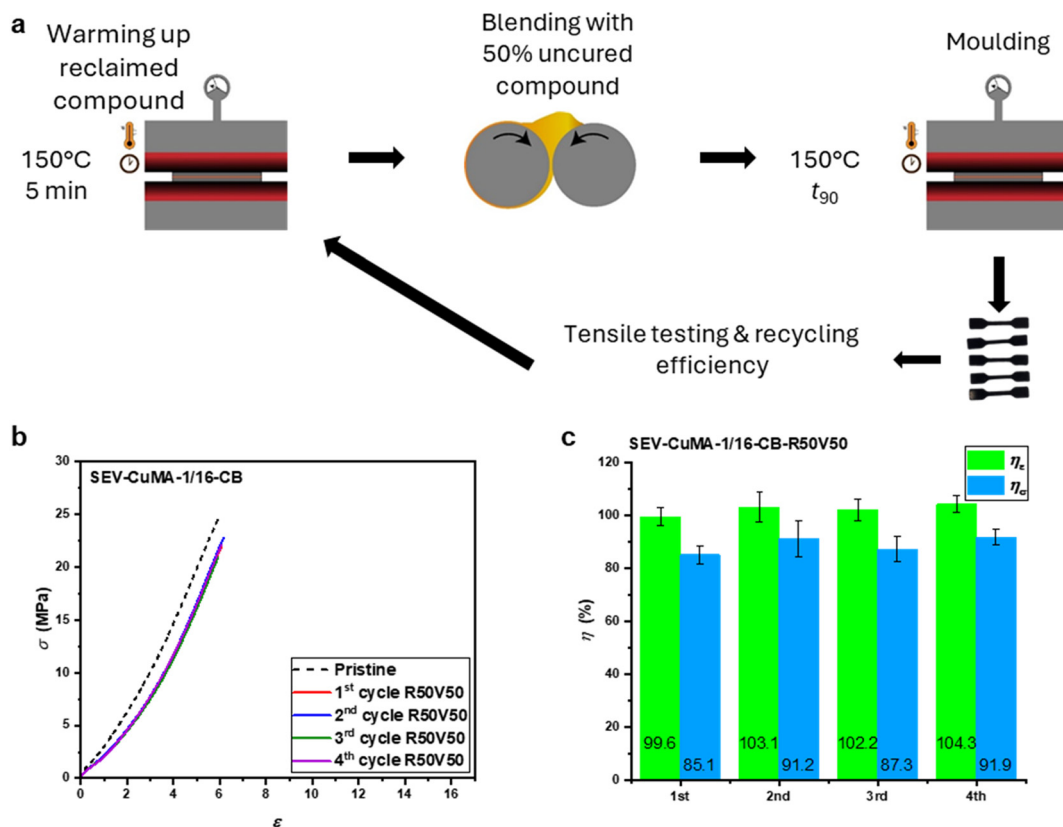


Fig. 7 (a) Schematics of repeated recycling events. Tensile properties of CB-filled recycled compound after multiple recycling events; (b) comparison of typical tensile test curves of pristine SEV-CuMA-1/16-CB (short dash black line) and four cycles of R50V50 (solid red line = 1st cycle, solid blue line = 2nd cycle; solid green line = 3rd cycle, solid purple line = 4th cycle); (c) recycling efficiencies in terms of stress and strain (green bars for  $\eta_\epsilon$ , blue bars for  $\eta_\sigma$ , standard deviation in solid black line).



Sombatsompop *et al.* produced a CV filled system capable of achieving 50% recovery of mechanical strength at a 40% recycle loading.<sup>25</sup> Seghar *et al.* achieved better performance of a recovery of 87% recovery of mechanical strength, however at a much lower recycle loading of 20% opposed to the 90% achieved herein.<sup>26</sup>

To validate the potential of SEV-CuMA-1/16-CB formulation to undergo several life cycles of usage, four recycling events were carried out in the form of R50V50, where in each cycle 50% of uncured compound was added to 50% of reclaimed compound (Fig. 7a).

The same initial drop in tensile strength previously seen in Fig. 6c is present for this testing as well, however beyond the initial drop, each further recycling event shows almost identical tensile stress *versus* strain plots. Future work will investigate alternative methodologies to understand if this initial drop can be mitigated including selective shear breakdown.<sup>15</sup> A maximum  $\epsilon$  of  $6.1 \pm 0.3$  and  $\sigma$  of  $24.6 \pm 0.6$  MPa was reached in the 2nd recycle, while the maximum  $\epsilon$  of  $6.0 \pm 0.2$  and  $\sigma$  of  $21.4 \pm 1.1$  MPa was achieved in the 3rd recycle, and the maximum  $\epsilon$  of  $6.2 \pm 0.1$  and  $\sigma$  of  $22.6 \pm 0.5$  MPa was reached in the 4th recycle (Fig. 7b).

These results suggest that after the initial softening, the formulation is capable of almost complete recyclability. It is

hypothesised that the initial changes to the polymer structure through the previously discussed potential route does not occur beyond the first recycling event, eventually reaching a steady state, with the 4th recycling event showing the highest homogeneity across the material as seen by the smallest standard deviation. This is also reflected in the recycling efficiency results, as  $\eta_\sigma$  of  $91.2 \pm 6.9\%$  and a  $\eta_\epsilon$  of  $103.1 \pm 5.7\%$  was reached in the 2nd cycle, a  $\eta_\sigma$  of  $87.3 \pm 4.8\%$  and a  $\eta_\epsilon$  of  $102.2 \pm 4.0\%$  was achieved in the 3rd cycle, and a  $\eta_\sigma$  of  $91.9 \pm 2.9\%$  and a  $\eta_\epsilon$  of  $104.3 \pm 3.2\%$  was reached in the 4th cycle (Fig. 7c).

As a way of investigating the potential of recycling existing waste, CuMA was introduced into reclaimed SEV-control-CB compound, by blending with 50% of uncured SEV-CuMA-1/16-CB.

The MDR analysis of the blended SEV-control-R50 + CuMA-1/16-V50-CB compound showed reasonable torque recovery compared to the pristine-cured SEV-control-CB compound, with a slight marching cure trace (Fig. 8a).

Additionally, partial recovery of the scorch time was observed in the blended compound. When looking at apparent crosslink density of the different compounds there was a good recovery of the crosslink density between SEV-control-CB and the blended compound, showing values of

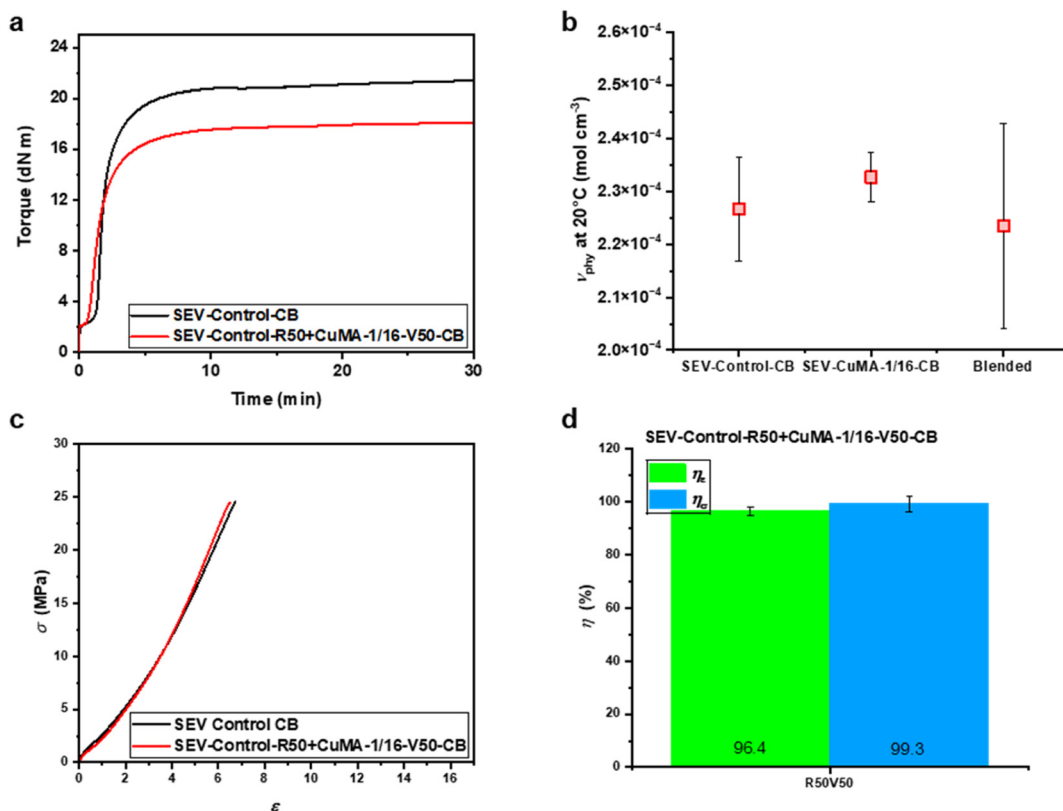


**Fig. 8** Curing characteristics of CB-filled blended compound SEV-control-R50 + CuMA-1/16-V50-CB. (a) Comparison between SEV-control-CB (solid black line) and SEV-control-R50 + CuMA-1/16-V50-CB (solid red line); (b) crosslinking density calculations for blend compound; tensile properties of CB-filled blended compound; (c) comparison of typical tensile test curves of pristine SEV-control-CB (solid black line) and SEV-control-R50 + CuMA-1/16-V50-CB (solid red line); (d) related recycling efficiencies (green bars for  $\eta_\epsilon$  and blue bars for  $\eta_\sigma$ , standard deviation in solid black line).



$2.27 \times 10^{-4} \pm 9.84 \times 10^{-6} \text{ mol cm}^{-3}$  and  $2.23 \times 10^{-4} \pm 1.94 \times 10^{-5} \text{ mol cm}^{-3}$  respectively.

The tensile properties of the blended SEV-control-R50 + CuMA-1/16-V50-CB compound showed almost complete recovery when compared to the pristine-cured SEV-control-CB compound, as maximum  $\epsilon$  of  $6.4 \pm 0.1$  and  $\sigma$  of  $24.0 \pm 0.5 \text{ MPa}$  was achieved (Fig. 8c), reporting a  $\eta_\sigma$  of  $99.3 \pm 3.0\%$  and a  $\eta_\epsilon$  of  $96.4 \pm 1.7\%$  respectively (Fig. 8d) significantly higher than when virgin material not including CuMA is utilised as the pristine component (Fig. 6b). Additionally, the low standard deviation reported suggests that good reproducibility was achieved. These results suggest that the recycling of previously vulcanised rubber without CuMA utilising, uncured compound with CuMA is possible.

### 3 Conclusions

Initial MDR analysis of the SEV compounds suggested that additional ratios of CuMA to disulphide bonds needed to be investigated due to a significantly reduced maximum torque for SEV-CuMA-1/1 and SEV-CuMA-1/2. SEV-CuMA-1/16 showed good torque recovery as well as reversion control after 30 min, but it also exhibited a very short scorch time. Mechanical testing of the recycled compounds and recycling efficiency calculations reported the most notable recovery of both the maximum tensile strength and elongation at break for SEV-CuMA-1/16. Further investigation into CB-filled compounds utilising 1/16 ratio of CuMA to disulphide bonds reported good recycling, as R90V10 reached a  $\eta_\sigma$  of  $85.0 \pm 3.2\%$  and a  $\eta_\epsilon$  of  $99.1 \pm 2.9\%$ , while R50V50 achieved a  $\eta_\sigma$  of  $85.1 \pm 3.4\%$  and a  $\eta_\epsilon$  of  $99.6 \pm 3.4\%$ .

These findings are particularly important as they indicate that high recyclability can be attained in CB-filled SEV formulations, which represents a predominant share of rubber materials used in commercial and industrial applications. Good recovery of both the maximum torque and scorch time was seen with SEV-CuMA-1/16-CB compound.

Significantly enhanced mechanical recovery was also achieved after four recycling events, with complete recovery of elongation at break achieved, with a slightly lower maximum mechanical strength after the 1st cycle. The ability

to incorporate the CuMA inhibitor into existing SEV-cured and CB-filled recycled waste was investigated by blending reclaimed SEV-control-CB compound with 50% of uncured SEV-CuMA-1/16-CB compound. This compound had a  $\eta_\sigma$  of  $99.3 \pm 3.0\%$  and a  $\eta_\epsilon$  of  $96.4 \pm 1.7\%$ . These results indicate that through the correct CuMA concentration, CB-filled systems can still achieve significant recycling efficiencies of the mechanical properties.

Despite this, there are several potential limitations towards industrial implementation, including a distinct drop in the ultimate tensile strength, resulting in materials showing a different tensile curve to the pristine materials, as well as a reduced scorch time limiting the range of potential processing methodologies available.

Therefore, further research into optimising the recycling conditions for these CuMA-based materials should be conducted, such as selective shear milling, to allow for complete recycling of commonly utilised formulations in almost all rubber applications. The recycling package could also be adjusted to account for the lowered scorch time, including addition of scorch retarders. Further investigation into why the CB filled compounds show a significant enhancement in the recycling efficiency when compared to the unfilled will be conducted in the future.

CuMA introduces  $\text{Cu}^{2+}$  centres that can coordinate to sulphur atoms in disulphide linkages present in the cross-linked rubber network. Although the S-S bond is relatively weak ( $\sim 240 \text{ kJ mol}^{-1}$ ), it is highly polarizable.<sup>27</sup> When  $\text{Cu}^{2+}$  is present, it can bind weakly to the lone pairs on sulphur, forming transient  $\text{Cu}\cdots\text{S}$  interactions that withdraw electron density from the S-S  $\sigma$  bond. This coordination reduces the nucleophilicity of sulphur and stabilises the disulphide bond, effectively raising the activation energy for S-S metathesis.

In the absence of  $\text{Cu}^{2+}$ , disulphide exchange can occur spontaneously at room temperature due to nucleophilic attack mechanisms (Fig. 9a). However, when  $\text{Cu}^{2+}$  is bound, these pathways are suppressed.<sup>17,28,29</sup> At higher temperatures, thermal energy can overcome this stabilization, allowing the S-S exchange to proceed again (Fig. 9b). This gives the network temperature-controlled dynamic behaviour: stable under service

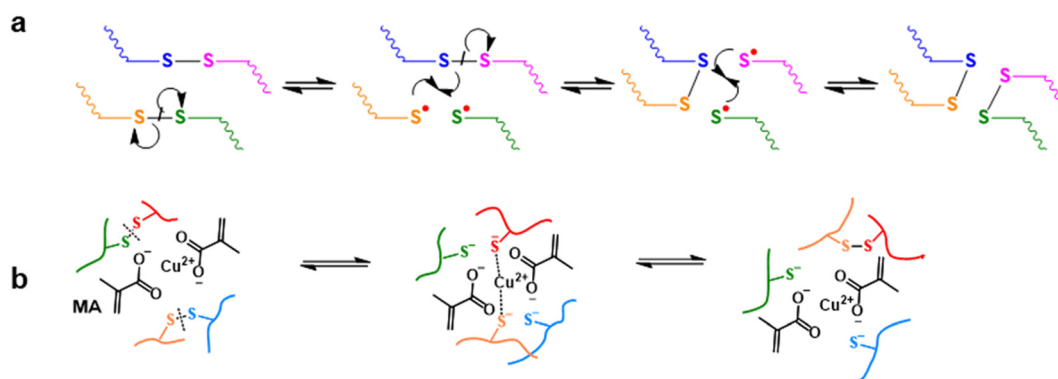


Fig. 9 Proposed mechanism of recyclability. (a) Reversibility of the disulphide bond, through radical formation and termination and (b) CuMA coordination with formed sulphur radicals.



conditions but reprocessable at elevated temperatures. It should be noted that this is a potential pathway for the increased recycling efficiency, therefore additional future work will investigate this hypothesis. Some potential pathways to investigate this includes the transformation of the sulphur crosslinks during the recycling event through means of sulphur probes measuring the proportions of each sulphur crosslink rank,<sup>30</sup> XPS analysis of the Cu 2p and S 2p binding energies,<sup>31</sup> or Raman spectroscopy to understand further the evolution of the disulphide bond.<sup>32</sup>

## 4 Experimental section

### 4.1 Materials

Natural rubber (NR, SMR CV60 grade) and *n*-cyclohexylbenzothiazol-2-sulphenamide (CBS) were purchased from Tun Abdul Razak Research Centre (TARRC) (United Kingdom). *N*-Isopropyl-*N'*-phenyl-*p*-phenylenediamine (IPPD; 95% purity) and sulphur (~325 mesh, 99.5% purity) were purchased from Alfa Aesar. Copper(II) methacrylate (CuMA, technical grade) was purchased from Fisher Scientific. Stearic acid (StA; 95% purity, reagent grade) and zinc oxide (ZnO; ≥98% purity, Light Technical grade) were purchased from VWR International Ltd. Toluene (≥99.9% purity, HPLC grade) was purchased from Honeywell International Inc. N330 carbon black (CB), 2,2,4-trimethyl-1,2-dihydroquinoline (TMQ) and tetramethylthiuram disulphide (TMTD) was supplied by TARRC.

### 4.2 Nomenclature

In the present work, SEV systems with and without CuMA and CB were formulated and tested in different conditions before and after curing and recycling. The terminology adopted to refer to the formulations in specific conditions is as follows:

- Uncured compound: virgin rubber compound that has been mixed but not cured.
- Pristine-cured compound: freshly cured compound.
- Reclaimed compound: material that, after vulcanisation, was collected for recycling.
- Recycled compound: recycled cured compound.
- Blended compound: recycled cured compound obtained by blending reclaimed SEV control compound with uncured SEV CuMA compound.

### 4.3 Preparation of unfilled rubber samples

Unfilled rubber formulations are reported in Table 1. NR was masticated in a laboratory two-roll mill for 5 min. StA was incorporated first (10–15 min) to minimise roll sticking, reduce the mixture viscosity and improve the mixing process. Subsequently, ZnO was gradually added (20–30 min), followed by IPPD (20–30 min). Once a homogenous mixture was obtained, CuMA was gradually added, with 10 min of mixing given per 1 gram of CuMA. Finally, CBS and sulphur were added, and the obtained uncured compound was moulded in a manual hot press at 150 °C, applying a constant pressure of about 12 MPa, for a curing time equal to

$t_{90}$  as reported in Table S1, determined using Monsanto Moving Die Rheometer (MDR) 2000 with the lower die moving at 1.66 Hz.

### 4.4 Preparation of filled rubber samples

The filled rubber formulations are reported in Table 1. NR was masticated in an OOC Banbury internal mixer for 2 min before ZnO, SA, TMQ and 6PPD and half the total CB amount was added. The mixture was mixed for 3 min before the remainder of CB was added with a further 3 min added for mixing. The resulting mixture was removed from the internal mixer at a dump temperature of 135 °C, and transferred to the two-roll mill, where sulphur, CBS and TMTD were added. The obtained uncured compound was moulded in a manual hot press at 150 °C, applying a constant pressure of about 12 MPa, for a curing time equal to  $t_{90}$  as reported in Table S2, determined using MDR 2000 with the central paddle moving at 1.66 Hz.

### 4.5 Recycling of rubber samples

To recycle the pristine compounds, they were heated in the hot press for 5 min at 150 °C and immediately masticated for at least five passes through the two-roll mill in which the rolls were at room temperature set to a gap of around 0.5 mm until a coarse granulate of around 1 mm diameter was obtained, seen in Fig. S1. The material was then blended with the same uncured rubber in the following mass fraction ratios (“R” stands for “reclaimed” and “V” stands for “virgin uncured”): 90% reclaimed rubber with 10% uncured rubber (R90V10); 80% reclaimed rubber with 20% uncured rubber (R80V20); 70% reclaimed rubber with 30% uncured rubber (R70V30); 50% reclaimed rubber with 50% uncured rubber (R50V50). The obtained blends were moulded in the manual hot press at 150 °C for the same time equal to the  $t_{90}$  to obtain the related pristine compound in Table S1 for unfilled and Table S2 for filled samples. For example: the time to mould a pristine SEV CuMA 1/4 compound is 8.3 min, so the time to mould SEV CuMA 1/4 R80V20 is also 8.3 min.

### 4.6 Density measurements

The density of NR and cured compounds was measured using a Micromeritics AccuPyc II 1345 gas-displacement pycnometer (number of purges 10, purge fill pressure 134.45 kPa, number of cycles 10, cycle fill pressure 134.45 kPa, equilibration rate 3.45 kPa min<sup>-1</sup>, chamber size 1 cm<sup>3</sup>). Three samples were measured for each compound.

### 4.7 Equilibrium swelling

Equilibrium swelling experiments were carried out in toluene and Flory–Rehner theory was applied to calculate the crosslink density,  $\nu_{\text{phy}}$  expressed in mol cm<sup>-3</sup>, of cured compounds following eqn (1):



$$v_{\text{phy}} = -\frac{\ln(1 - V_E) + V_E + \zeta V_E^2}{v_0(V_3^{1/3} - \frac{V_E}{2})} \quad (1)$$

$$\varepsilon = \frac{\Delta L}{L_0} \quad (5)$$

where  $v_0$  is the molar volume of the swelling liquid,  $\zeta$  is the Flory–Rehner interaction parameter and  $V_E$  is the volume fraction of the polymer in the mixture. A dry and rectangular shape sample for each cured compound was weighed and then immersed in a vial containing excess toluene (approximately 0.2 g of rubber in 20 mL of Toluene). The vials were then left in a dark environment for 14 days.

After this time, the sample was removed from the solution, the surfaces were tap dried on a white lint-free tissue and weighed again. The sample was then dried under reduced pressure to remove the solvent and then weighed a third time. The experiment was repeated three times for each cured compound. The Flory–Rehner interaction parameter for NR–toluene interaction is 0.385, while  $v_0$  for toluene is 106.28 cm<sup>3</sup>. To calculate  $V_E$  the following eqn (2) is used:

$$V_E = \frac{V_{\text{EN}}}{V_{\text{EN}} + V_S} \quad (2)$$

where  $V_S$  is the volume of the solvent absorbed and  $V_{\text{EN}}$  is the volume of elastomer network, which can be determined following eqn (3):

$$V_{\text{EN}} = \frac{m_{\text{EN}}}{m_{\text{tot}}} \cdot \frac{m_0}{\rho_E} \quad (3)$$

where  $\rho_E$  is the density of the cross-linked polymer,  $m_{\text{EN}}$  is the mass of the rubber and cross-linker used in the whole formulation, whose  $m_{\text{tot}}$  is the total weight and  $m_0$  is the weight of the dried sample after swelling. It should be noted that for the filled system, the crosslink density found using eqn (1) will not be the real crosslink density as fillers do not swell or can act as additional crosslinks. The values achieved will be used as a comparative crosslink density, denoted as the apparent crosslink density, as each compound has the same filler type and loading.

#### 4.8 Tensile testing

Tensile testing until failure at room temperature was carried out on cured compounds. Dumbbell shape samples were cut out using an ISO-37-4 die cutter 24 hours after curing was completed. Testing was conducted using an Instron 68TM-10 machine equipped with a 2 kN load cell and pneumatic side action grips, using a rate of 1 mm s<sup>-1</sup>. The width (2.02 ± 0.07 mm) and the thickness (1.82 ± 0.08 mm) were measured prior to the start of the test while the initial length,  $L_0$  (11.21 ± 1.24 mm), was measured after gripping the sample, ensuring the width of the sample remained constant in the gauge length. Uniaxial stress,  $\sigma$ , and strain,  $\varepsilon$ , were calculated using the following eqn (4) and (5):

$$\sigma = \frac{F}{A_0} \quad (4)$$

where  $F$  is the measured force,  $A_0$  is the initial unstrained cross-sectional area, and  $\Delta L$  the measured elongation. Tests were repeated until failure 5 times for each cured compound.

#### 4.9 Recycling efficiency

Recycling efficiency in terms of stress,  $\eta_\sigma$ , was calculated by comparing the ultimate tensile strength of pristine compounds and recycled compounds using eqn (6):

$$\eta_\sigma = \frac{\sigma_{\text{recycled}}}{\sigma_{\text{pristine}}} \cdot 100 \quad (6)$$

The recycling efficiency in terms of strain,  $\eta_\varepsilon$ , was calculated by comparing the ultimate tensile strain of pristine compounds and recycled compounds using eqn (7):

$$\eta_\varepsilon = \frac{\varepsilon_{\text{recycled}}}{\varepsilon_{\text{pristine}}} \cdot 100 \quad (7)$$

## Statistical information

Crosslink density calculations were carried out on three samples with the averages obtained and the standard deviation reported. Tensile testing for pristine, recycled and blended compounds was repeated a minimum of 5 times for samples containing CuMA and a minimum of three times for samples without CuMA. The experimental data shown is therefore the mean of these values with the standard deviation reported. While the curves plotted in figures are a representative curve chosen from the repeats.

## Author contributions

All authors have read and approved the final manuscript. Thomas Griggs and Anureet Kaur conceived the research idea and designed the experimental methodology, performed analysis and data interpretation, drafted the initial paper and incorporated feedback from co-authors; Meet M. Fefar contributed by conducting part of the laboratory experiments and collecting relevant data; Keizo Akutagawa played a key role in discussing and refining the theoretical framework and implications of the findings; Biqiong Chen, Ton Peijs, and James J. C. Busfield jointly secured research funding and reviewed the data and supported the interpretation; James J. C. Busfield supervised this work and provided access to specialised equipment and facilities. All authors discussed the results and commented on the manuscript.

## Conflicts of interest

The authors declare no conflict of interest.



## Data availability

All data (MDR, GPC, DSC, tensile stress–stretch, swelling) is available from the Queen Mary University of London open access repository through the following link: <https://qmro.qmul.ac.uk/xmlui/handle/123456789/126556>.

Supplementary information (SI) is available. See DOI: <https://doi.org/10.1039/d5im00385g>.

## Acknowledgements

The work was supported by the Engineering and Physical Sciences Research Council (EPSRC) grant EP/W018977/1.

## References

- 1 ANRPC revises up natural rubber demand in 2024, <https://www.european-rubber-journal.com/article/2094013/anrpc-revises-up-natural-rubber-supply-demand>, (December 2025).
- 2 Rubber – Statistics & Facts, Statista, <https://www.statista.com/topics/3268/rubber/>.
- 3 Will rubber prices continue their slide from seven-year highs this year?, Int. Banker, <https://internationalbanker.com/brokerage/will-rubber-prices-continue-their-slide-from-seven-year-highs-this-year/>.
- 4 Environmental Impact of Rubber – Sustainability Matters, Ball Science, <https://ballscience.net/environmental-impact-of-rubber-sustainability-matters/>.
- 5 Natural Rubber Supply Chain, European Tyre & Rubber Manufacturers' Association, 2022, <https://www.etrma.org/key-topics/materials/natural-rubber/>.
- 6 Y. Liu, H. Chen, S. Wu, J. Gao, Y. Li, Z. An, B. Mao, R. Tu and T. Li, Impact of vehicle type, tyre feature and driving behaviour on tyre wear under real-world driving conditions, *Sci. Total Environ.*, 2022, **842**, 156950.
- 7 J. D. Martínez, N. Puy, R. Murillo, T. García, M. V. Navarro and A. M. Mastral, Waste tyre pyrolysis – A review, *Renewable Sustainable Energy Rev.*, 2013, **23**, 179–213.
- 8 T. Amari, N. J. Themelis and I. K. Wernick, Resource recovery from used rubber tires, *Resour. Policy*, 1999, **25**, 179–188.
- 9 P. J. H. van Beukering and M. A. Janssen, Trade and recycling of used tyres in Western and Eastern Europe, *Resour., Conserv. Recycl.*, 2001, **33**, 235–265.
- 10 N. Flores Medina, R. Garcia, I. Hajirasouliha, K. Pilakoutas, M. Guadagnini and S. Raffoul, Composites with recycled rubber aggregates: Properties and opportunities in construction, *Constr. Build. Mater.*, 2018, **188**, 884–897.
- 11 T. Moreno, A. Balasch, R. Bartrolí and E. Eljarrat, A new look at rubber recycling and recreational surfaces: The inorganic and OPE chemistry of vulcanised elastomers used in playgrounds and sports facilities, *Sci. Total Environ.*, 2023, **868**, 161648.
- 12 M. Kojima, K. Ogawa, H. Mizushima, M. Tosaka, S. Kohjiya and Y. Ikeda, Devulcanization of sulfur-cured isoprene rubber in supercritical carbon dioxide, *Rubber Chem. Technol.*, 2003, **76**, 957–968.
- 13 A. Pelofsky, *US Pat.*, 3725314, 1973.
- 14 C. H. Scuracchio, D. A. Waki and M. L. C. P. da Silva, Thermal analysis of ground tire rubber devulcanized by microwaves, *J. Therm. Anal. Calorim.*, 2007, **87**, 893–897.
- 15 J. R. Innes, N. Siddique, G. Thompson, X. Wang, P. Coates and B. Whiteside, *et al.*, The influence of devulcanization and revulcanization on sulfur cross-link type/rank: Recycling of ground tire rubber, *ACS Omega*, 2024, **9**, 29175–29188.
- 16 L. Gonzalez, A. Rodriguez, J. L. Valentin, A. Marcos-Fernández and P. Posadas, *Conventional and efficient crosslinking of natural rubber*, KGK Rubberpoint, 2005, vol. 58, pp. 638–646.
- 17 A. Kaur, M. M. Fefar, T. Griggs, K. Akutagawa, B. Chen and J. J. C. Busfield, Recyclable sulfur cured natural rubber with controlled disulfide metathesis, *Commun. Mater.*, 2024, **5**, 212.
- 18 W. A. Kyei-Manu, C. R. Herd, M. Chowdhury, J. J. C. Busfield and L. B. Tunnicliffe, The influence of colloidal properties of carbon black on static and dynamic mechanical properties of natural rubber, *Polymers*, 2022, **14**, 1194.
- 19 C. G. Moore and B. R. Trego, Structural characterization of vulcanizates. Part IV. Use of triphenylphosphine and sodium di-n-butyl phosphite to determine the structures of sulfur linkages in natural rubber, cis-1,4-polyisoprene, and ethylene-propylene rubber vulcanizate networks, *J. Appl. Polym. Sci.*, 1964, **8**, 1957–1983.
- 20 P. Kumar, Y. Fukahori, A. G. Thomas and J. J. C. Busfield, Volume changes under strain resulting from the incorporation of rubber granulates into a rubber matrix, *J. Polym. Sci., Part B: Polym. Phys.*, 2007, **45**, 3169–3180.
- 21 E. H. Plaschka, K. Akutagawa, E. Di Federico and J. J. C. Busfield, Developing a more representative friction and wear simulator for tire tread compounds, *Polym. Test.*, 2025, **128**, 108688.
- 22 E. Koliolios, S. Nakano, T. Kawamura and J. J. C. Busfield, Elucidation of smear wear layer structure and ageing mechanisms of filled tyre tread compounds, *Polymer*, 2024, **300**, 126982.
- 23 T. L. M. Baumard, A. G. Thomas and J. J. C. Busfield, Fatigue peeling at rubber interfaces, *Plast., Rubber Compos.*, 2012, **41**, 296–300.
- 24 J. M. Peña, N. S. Allen, M. Edge, C. M. Liauw, S. R. Hoon, B. Valange and R. I. Cherry, Analysis of radical content on carbon black pigments by electron spin resonance: influence of functionality, thermal treatment and adsorption of acidic and basic probes, *Polym. Degrad. Stab.*, 2000, **71**, 153–170.
- 25 N. Sombatsompop and C. Kumnuantip, Rheology, cure characteristics, physical and mechanical properties of tire tread reclaimed rubber/natural rubber compounds, *J. Appl. Polym. Sci.*, 2003, **87**, 1723–1731.
- 26 S. Seghar, L. Asaro, M. Rolland-Monnet and N. Aït Hocine, Thermo-mechanical devulcanization and recycling of rubber industry waste, *Resour., Conserv. Recycl.*, 2019, **144**, 180–186.
- 27 R. J. Cremllyn, *An Introduction to Organosulfur Chemistry*, John Wiley & Sons, 1996.
- 28 S. Li, P. Tan, J. Cao, Y. Yao, X. Ren and Y.-X. Xu, High performance, self-healing and recyclable polyisoprene rubbers enabled by modulating sulfide bond structures, *Polymer*, 2025, **332**, 128570.



- 29 J. Cao, S. Li, C.-C. Wang, R. Xu, M. Tang, X. Ren and Y.-X. Xu, Recyclable sulfur-cured rubbers with enhanced creep resistance and retained mechanical properties by terminal metal coordination, *Ind. Eng. Chem. Res.*, 2022, **61**, 11727–11734.
- 30 S.-S. Choi and E. Kim, A novel system for measurement of types and densities of sulfur crosslinks of a filled rubber vulcanizate, *Polym. Test.*, 2015, **42**, 62–68.
- 31 G. E. Hammer, X-ray photoelectron spectroscopy of rubber compounds: Temperature dependence and cross-link distribution, *J. Vac. Sci. Technol., A*, 2007, **25**, 1599–1603.
- 32 G. Butuc, K. van Leerdam, B. Rossenaar, A. Talma and A. Blume, Deciphering the crosslink mechanism of dual cure EP(D)M and CTS rubber compounds for reduced oil swell, *Polym. Test.*, 2025, **145**, 108736.

